Journal of Fluorescence (2019) 29:819–825
https://doi.org/10.1007/s10895-019-02408-x

FLUORESCENCE NEWS ARTICLE

Fluorescence "Off-On" Probe for L-Cysteine Detection Based on Nitrogen Doped Carbon Dots

Yin-long Xu[1] · Rong-biao Bai[1] · Cai-yu Qi[1] · Zeng Ren[2] · Xiu-zhi Jia[3] · Zi-gui Kan[1] · Cao-long Li[1,2] · Fei Wang[1]

Published online: 18 July 2019

Abstract

Herein, a simple and efficient fluorescence analysis method for L-Cysteine (L-Cys) was established. The method was based on the fluorescent "off-on" mode of nitrogen doped carbon dots (NCDs). The NCDs were prepared via a facile one-step solvothermal method. In the process of exploring the bio-functional application of these newly synthesized NCDs, we found these NCDs with rich functional groups exhibited excellent optical properties. In addition, these newly synthesized NCDs showed an excitation-dependent emissions photolumine-scent (PL) property and exhibited good performance in the detection of Fe^{3+} ions by quenching the blue emission fluorescence. Interestingly, the quenched fluorescence of NCDs was recovered with the addition of L-Cys, which provided a novel approach for L-Cys detection. The NCDs-based fluorescent "off-on" sensor has a wide linear detection range (0–100 μM), and a relatively low detection limits (0.35 μM) for L-Cys. This simple fluorescent "off-on" approach is, very sensitive and selective for L-Cys detection, which also provides a new insight on NCDs biosensor application.

Keywords Carbon dots · Solvothermal · Fluorescence "off-on" probe · L-Cys detection

Introduction

Sulfhydryl-containing amino acids play a unique and important role in the process of biological metabolism, which has received extensive attentions in the biological research [1–3]. Multifarious diseases are closely related to amino acid content since amino acids are crucial component of proteins and various metabolites [4]. Among these amino acids, L-Cysteine (L-Cys), serving as one of 20 essential amino acids and an important sulfur-containing compound, plays an extensive role in human physiological activities [5, 6]. L-Cys deficiency is usually associated with retarded growth in children, leukocyte loss, skin lesions, liver damage, and weakness [7]. In addition, L-Cys is also used in pharmaceuticals, cosmetics, baking and as a flavoring additive in industrial application [8]. Therefore, the ability to accurately detect L-Cys level in a variety of products is essential.

In the past decades, atomic absorption spectrometry, high-performance liquid chro-matography (HPLC), optical spectroscopy, the electrochemical and chemical methods have been applied to monitor L-Cys levels [9–11]. However, those methods require harsh conditions, sophisticated operations, relatively expensive equipment and time-consuming pretreatments. Compared to these traditional methods, fluorescence detection methods attracted extensive attention due to quick response, high sensitivity, and high selectivity. Among them, fluorescent turn-on probes are particularly preferred to avoid the false response and to enhance the visible distinguishability [12, 13].

Nanomaterials are used as fluorescent probes, such as gold and silver nanoparticles, CdS quantum dots, graphene quantum dots and carbon dots (CDs). Compared with other

Electronic supplementary material The online version of this article (https://doi.org/10.1007/s10895-019-02408-x) contains supplementary material, which is available to authorized users.

✉ Cao-long Li
licl@cpu.edu.cn

✉ Fei Wang
feiwang@cpu.edu.cn

[1] Key Laboratory of Biomedical Functional Materials, School of Basic Science, China Pharmaceutical University, Nanjing 211198, People's Republic of China

[2] Tibetan Medicine Research Institute, Tibetan Traditional Medical College, Tibet 850000, People's Republic of China

[3] School of Basic Medical Science, Harbin Medical University, Harbin 150081, China

nanomaterials, CDs not only possess good biocompatibility, catalytic activity and optical properties, but also show advantages in the simple preparation processes, lower toxicity and higher stability [14–16]. In recent years, CDs have attracted tremendous attention in catalysts [17], sensors [18–20], printing inks [21], optoelectronic devices [22] and theranostics [23, 24] and bioimaging [25–27]. In addition, researches showed that heteroatom doping were widely used to improve the fluorescence emission performance of CDs and provide extra functional groups for specific targeted sensing [28–31]. The various metal ions can chelate with functional groups, resulting in the fluorescence quenching of CDs, which was used to detect metals ions (Cu^{2+}, Hg^{2+}, Cr^{6+}, Fe^{3+}) [1–3, 32].

Alternatively, a sensitive and specific fluorescence "off-on" mode for determination of L-Cys has been studied, which further expanded the applications of CDs. The fluorescent probes for "off-on" sensor have been applied to detect L-Cys level based on CDs- Cu^{2+} and CDs- Ag^{+} fluorescence [1, 33]. The methods in the form of "on - off - on" by first quenching the fluorescence of CDs with metal ions and then recovering the fluorescence with the addition of L-Cys are a relatively cheap, facile, quick response and selective approach. Therefore, in order to further develop the fluorescent probes method, we designed a novel fluorescence "off-on" sensors for L-Cys detection based on NCDs-Fe^{3+}.

The NCDs with good stability and excellent optical properties were prepared by a one-step solvothermal method with 4-(2-pyridylazo)-resorcinol as carbon precursor. In addition, the blue fluorescence quenching could not only be ascribed to the combination of Fe^{3+} ions and the rich functional groups on the surface of the NCDs, but the fluorescence of NCDs was recovered with the addition of L-Cys, which was used to detect L-Cys detection based on fluorescence "off-on" probes. Moreover, compared with the previously reported probes, the NCDs-based fluorescent "off-on" sensor has a wide linear detection range (0–100 μM) and a relatively low detection limits (0.35 μM) for L-Cys detection.

Materials and Methods

Reagents and Materials

4-(2-Pyridylazo)-resorcinol was acquired from Macklin Biochemical Co., Ltd. (Shanghai). Ethanol, methanol and methylene chloride were purchased by Sinopharm Chemical Reagent Co., Ltd. (Shanghai). L-Cys and all amino acids were obtained from Aladdin Industrial Inc. (Shanghai, China). Ultra-pure water was prepared and used throughout the whole experiments.

Instrumentation and Characterization

Fluorescence emission spectra of the samples were measured by using the Fluomax-4 Spectrophotometer at ambient conditions. Fourier transform infrared (FT-IR) spectroscopy were obtained on a Nicolet Nexus 670 FTIR spectrometer ranged from 4000 to 400 cm^{-1}. UV − visible absorption spectra were collected using a Shimadzu UV-2600 spectrophotometer. Transmission electron microscopy (TEM) images were captured using a Tecnai G2 20 transmission electron microscope. The measurements of C, H, and N elements were performed on Agilent 7700ce elemental analyzer.

Preparation of NCDs

The NCDs were synthesized by a one-step solvothermal method. 4-(2-pyridylazo)-resor-cinol (0.15 g) was first dissolved in ethanol (80 mL). The mixture solution was transferred into multiple poly-(tetrafluoroethylene)-lined auto-claves for solvothermal reaction. The reactors were then heated at 220 °C for 10 h and cooled naturally to room temperature. The obtained crude products were preliminarily purified by high-speed centrifuged and further filtered through a filter membrane (0.22 μm) to remove the large particle residues. The flow-through was purified on a silica-column using methanol and methylene chloride mixtures (1:4, *v*/v) as the eluent. After removing solvents using rotary evaporator at 50 °C and further drying in a 50 °C vacuum oven for 10 h, the final purified NCDs were obtained as a dark powder.

Detection of L-Cys

The detection of L-Cys was performed following a typical procedure. First, 3 ml of ethanol solution containing 60 μg NCDs were mixed with certain Fe^{3+} ions (500 μM) solution, which was denoted as NCDs-Fe^{3+}. Subsequently, various concentration of L-Cys (0–500 μM) were added to NCDs-Fe^{3+}. Finally, the fluorescence emission spectra was then measured with excitation wavelength fixed at 350 nm.

Results and Discussions

Morphological and Chemical Characteriz-Ation of NCDs

The synthesis of NCDs started from 4-(2-pyridylazo)-resorcinol through a facile one-step solvothermal method using ethanol as solvent. Subsequently, the morphology and size distribution of as-prepared NCDs were characterized using TEM to confirm the properties of nanoparticles. The TEM image of the NCDs revealed that NCDs were monodispersed nanoparticles and quasi-spherical with an average diameter

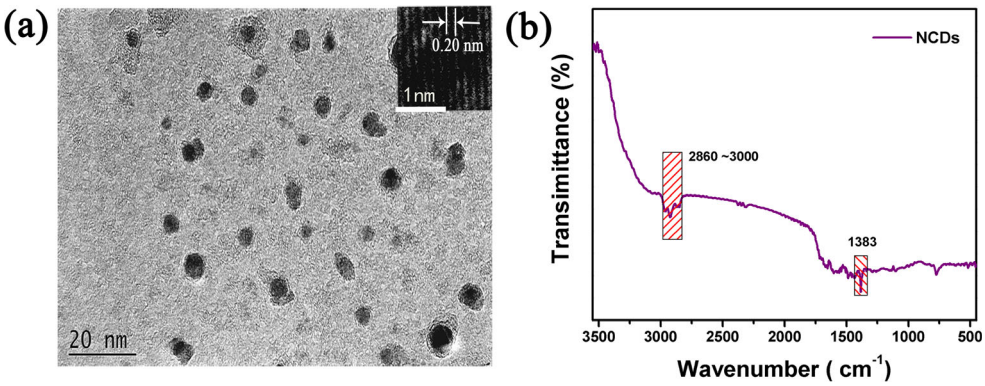

Fig. 1 **a** TEM images, **b** FT-IR spectra of NCDs and precursors. Inset in (**a**): the lattice fringes of NCDs from HRTEM observation

about 4.99 nm (Fig. 1a). HRTEM image exhibited the clear lattice structures with fringe spacing of 0.20 nm, which was ascribed to the (100) facet of grapheme [34, 35]. The surface states and composition of as-prepared NCDs were analyzed by FT-IR and Elemental analysis (EA). As shown in the FT-IR spectra of NCDs (Fig. 1b), the peaks between 2850 and 3000 cm^{-1} of NCDs corresponded to C − H stretching vibrations. In addition, the peaks at around 1500 cm^{-1} and 1383 cm^{-1} were arising from C=C and C − N = stretching vibrations, respectively, which suggested that the NCDs core was composed of poly-aromatic structures [36, 37]. Furthermore, Elemental analysis (EA) demonstrated that NCDs was composed of three elements: carbon, nitrogen and oxygen and the atomic ratio of C/N/O was 1/0.17/0.36 (Table S1). XPS data showed that NCDs contained abundant nitrogen and oxygen functional groups, which were consistent with FT-IR results (Figure S1). The synergistic effect of nitrogen- and oxygen-related surface states and nitrogen-derived structures in carbon cores were beneficial to the application of NCDs in sensing [38].

Optical Properties of NCDs

The optical properties of the synthesized NCDs were assessed with UV-vis absorption and FL spectra. The UV-vis absorption spectra of the NCDs exhibited two new absorption peaks at 241 and 290 nm in Fig. 1c (red line), which were ascribed to the π − π* transition of C=C and C=N bonds of the aromatic rings, respectively [39, 40]. In comparison to the starting materials, the UV-vis absorption spectra of the NCDs blue-shift (Figure S2), which demonstrated that the NCDs should contain bigger electronic band gaps than 4-(2-pyridylazo)-resorcinol. Then, the PL properties of the NCDs were thoroughly investigated by FL spectra. Like most previously reported CDs, the new synthesized NCDs showed excitation-dependent features (Figure S3), which could be attributed to the surface state of NCDs. Moreover, the NCDs exhibited relatively high absolute fluorescence quantum yield (QY = 11.6%) based on quinine sulphate (Table S2). To investigate the fluorescence stability, various conditions were studied, such as different pH values, UV irradiation time changes and the different ionic concentrations of the solutions (Figure S4–7). The confirmative fluorescence stability results support the potential app-lications of the new synthesized NCDs in various conditions.

Detection of L-Cys

The NCDs have great potentials in sensing applications due to the abundant functional groups on the surface. Through broadly screening, NCDs displayed a significant “on-off-on” three-state emission when Fe^{3+} and L-Cys was added in

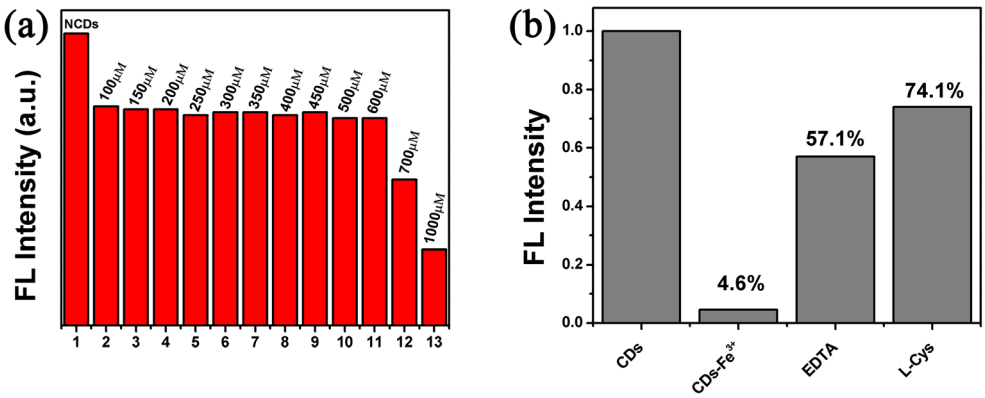

Fig. 2 **a** The fluorescence intensity of the NCDs with the different concentrations of Fe^{3+} ions, and then L-Cys (1 mM) was added. **b** The fluorescence intensity of the NCDs, NCDs-Fe^{3+}, NCDs- Fe^{3+}-EDTA, NCDs Fe^{3+}-L-Cys

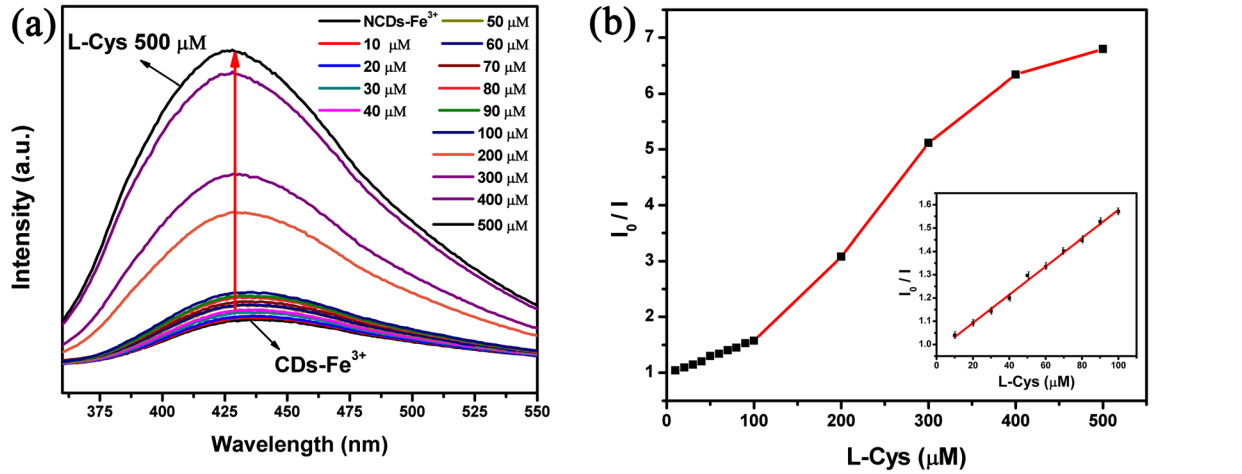

Fig. 3 **a** Fluorescence titration curve of the NCDs - Fe^{3+} with concentrations of L-Cys ions from 0 to 500 μM. **b** PL emission change of NCDs with different concentrations of L-Cys, where I and I_0 are the fluorescence intensity of NCDs - Fe^{3+} before and after adding of L-Cys. Inset in (**b**): Linear Relationship of Fluorescence Intensity NCDs - Fe^{3+} with L-Cys (0-100 μM)

sequence, respectively. The Fe^{3+} ions had a strong quenching effect on the fluorescence through facilitating charge transfer from the excited state of the NCDs to metal ions. Moreover, other metal ions have no effect on the fluorescence intensity of NCDs (Figure S8). In addition, the fluorescence of the NCDs was recovered with the addition of L-Cys due to the stronger chelation effects of Fe^{3+} ions and L-Cys [41–43]. These findings make the NCDs a potentially functional sensing platform for the detection of L-Cys.

The fluorescent sensing assay were performed to investigate the sensitivity of the NCDs toward L-Cys. In order to obtain the best sensing response, the different concentrations of Fe^{3+} ions were optimized systematically. First, the various concentrations of Fe^{3+} ions were mixed with NCDs and then L-Cys (1 mM) was added. The fluorescence intensity recovery reduced significantly when the concentration of Fe^{3+} ions exceeded 600 μM (Fig. 2a). The extra Fe^{3+} ions react with L-Cys when the concentration of Fe^{3+} is higher, which interferes with L-Cys detection. The linear range became smaller when the concentration of Fe^{3+} ions is less. The fluorescence intensity quenching effect of NCDs reached 95.4% when the Fe^{3+} ion concentration was 500 μM (Figure S9). In addition, compared with the traditional complexion agent EDTA, L-Cys showed better performance to Fe^{3+} ions under similar conditions (Fig. 2b). Therefore, 500 μM Fe^{3+} ions were selected to bond to the NCDs. The quenched fluorescence was immediately turned on when L-Cys was added to the mixed solution of NCDs-Fe^{3+}. As shown in Fig. 3a, the fluorescence intensity of NCDs-Fe^{3+} continuously increases with the addition of different concentration of L-Cys. The good linear relationship for fluorescence enhan-cement is established when the concentration of L-Cys is in the range of 0–100 μM (Fig. 3b). In addition, the fitted linear regression equation is $I_0/I = 6.07 \times 10^3$ [L-Cys] (μM) + 0.97. The fluorescence

Table 1 Comparison of different probes for the sensing of L-Cys

Methods	Probes	Linear range (μM)	Detection limit (μM)	Reference
Fluorimetry	Amino nitrogen quantum dots–gold nanoparticles	0.3–3.0	0.1	[44]
Fluorimetry	RhB@Cu-BTC	0–40.0	0.702	[45]
Fluorimetry	ESIPT dye	30–200	0.80	[46]
Fluorimetry	Tyrosine-functioalized $CuInS_2$ quantum dots–Cu^{2+}	1–50	0.5	[47]
Absorption	Cinamaldehyde and pyrimidine–Hg^{2+}	0.1–5	0.1	[48]
Fluorimetry	CQDs–Hg^{2+}	0.2–45	0.05	[49]
Fluorimetry	N-CQDs–Hg2+	0–70	45.8	[50]
Fluorimetry	S,N-CQDs–Ag^{+}	0–10 and 10–120	0.35	[37]
Fluorimetry	y-CDs – Ag+	2–10	0.25	[51]
Fluorimetry	NCDs–Fe^{3+}	0–100	0.35	This work

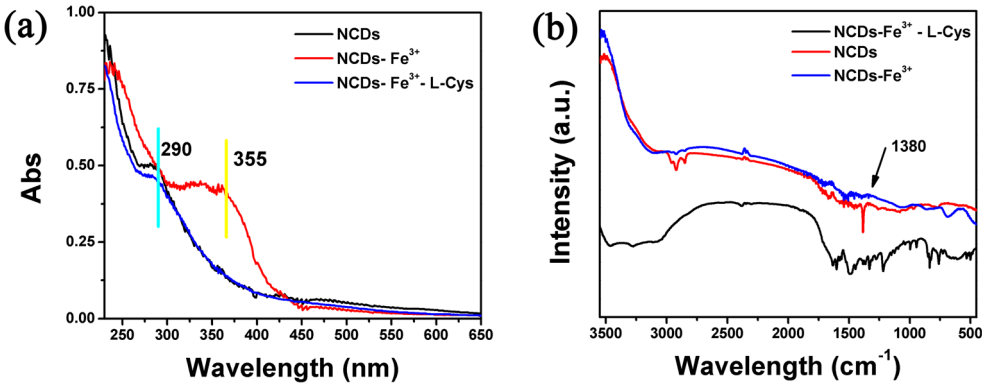

Fig. 4 UV − vis absorption spectrum of the NCDs, NCDs-Fe^{3+} and NCDs-Fe^{3+}- L-Cys (**a**). FT-IR spectra of NCDs, NCDs-Fe^{3+} and NCDs-Fe^{3+} − L-Cys (**b**)

enhancement could be also described by the Stern–Volmer equation: $I_0/I = 1 + K_{sv}$ [Q], where [Q], K_{sv}, I_0 and I represent the concentration of L-Cys, the Stern–Volmer constant, fluorescence inten-sities of NCDs-Fe^{3+} in the absence and presence of L-Cys, respectively. Based on the three times signal-to-noise criteria, the detection limit of L-Cys is calculated to be 0.35 μM, which indicates that fluorescence detection method has ultra-high sensitivity. Compared with other amino acids, L-Cys has obvious recovery effect on fluorescence of NCDs (Figure S10). The NCDs-based fluores-cent "off-on" sensor for L-Cys detection not only has a relatively low detection limit, but also has a wide linear range compared with the previously reported methods (Table 1) [37, 44–51].

Mechanism of the "Off–On" Detection of L-Cys

NCDs displayed a significant "on-off-on" three-state emission when Fe^{3+} and L-Cys was added in sequence, respectively. The mecha-nism of the "off–on" fluorescent probes for determination of L-Cys based on NCDs was showed as Scheme S1. The mechanism was explored by ultraviolet visible and infrared spectra. First, in the ultraviolet visible spectrum, the absorption peak of NCDs at 290 nm had red-shifted to 355 nm with the addition of Fe^{3+} ions, which was due to the chelation between Fe^{3+} ions and functional groups NCDs (Fig. 4a). In addition, the red-shifts of the electronic absorption transitions demonstrated that the NCDs-Fe^{3+} should contain smaller electronic band gaps than NCDs due to facilitate charge transfer from the excited state of the NCDs to Fe^{3+} ions. Then, the absorption peak of NCDs at 290 nm appeared again when L-Cys was added, which showed that L-Cys and Fe^{3+} ions had stronger binding (Fig. 4a). In addition, compared to the NCDs, the peak intensity of NCDs - Fe^{3+} ions reduced at 1380 nm in the infrared spectrum, which indicating that Fe^{3+} ions interacted with the C- N/ C = N bond on the surface of NCDs. Then, the Fe^{3+} ions were separated from the surface of NCDs when L-Cys was added and the peak at 1380 nm appeared again, which implied the stronger chelation effects of Fe^{3+} ions and L-Cys (Fig. 4b).

Conclusions

In summary, the as-prepared NCDs exhibited not only excellent monodispersity, higher stability and storage stability but also the simple preparation processes, catalytic activity and optical properties. In addition, Fe^{3+} ions could quench the fluorescence of NCDs due to interact with the C - N / C = N bond on the surface of NCDs. The fluorescence was again recovered with the addition of L-Cys into NCDs-Fe^{3+}, which was attributed to the stronger chelation effects of Fe^{3+} ions and the thiol group of L-Cys. Therefore, the fluorescent probe for "off-on" sensor is achieved to detect L-Cys based on NCDs-Fe^{3+}. The method in the form of "on - off - on" by first quenching the fluorescence of NCDs using Fe^{3+} ions and then recovering the fluorescence with the addition of L-Cys, is a relatively cheap, facile, quick response and environmental friendly. Moreover, the fluore-scent "off-on" sensor not only has a wide linear range of detection (0–100 μM), but also has a relatively low detection limit for L-Cys (0.35 μM). The NCDs based fluorescent probe we developed provided a new approach for desirable biosensor applications.

Acknowledgements Great appreciate to financial support by the National Natural Science Foundation of China (81660708) and Natural Science Foundation of Jiangsu Province of China (BK20171389). The work is also sponsored by the Qinglan Project of Young Academic Leaders of Jiangsu Province, the Key Project of Science and Technology of Tibet (2015XZ01G70) and the Key Project of Tibetan Medical Administration of Tibet (2017005).

References

1. Zong J, Yang XL, Trinchi A, Hardin S, Cole I, Zhu YH, Li CZ, Muster T, Wei G (2014) Carbon dots as fluorescent probes for "off-on" detection of Cu^{2+} and L-cysteine in aqueous solution. Biosens Bioelectron 51
2. Li Z, Wang Y, Ni YN, Kokot S (2015) A rapid and label-free dual detection of Hg (II) and cysteine with the use of fluorescence switching of graphene quantum dots. Sensors Actuators B Chem 207
3. Zhou L, Lin YH, Huang ZZ, Ren JS, Qu XG (2012) Carbon nanodots as fluorescence probes for rapid, sensitive, and label-

free detection of Hg^{2+} and biothiols in complex matrices. Chem Commun 48(8)
4. Zhang MM, Saha ML, Wang M, Zhou ZX, Song B, Lu CJ, Yan XZ, Li XP, Huang FH, Yin SC, Stang PJ (2017) Multicomponent platinum(II) cages with tunable emission and amino acid sensing. J Am Chem Soc 139(14)
5. Wei LF, Thirumalaivasan N, Liao YC, Wu SP (2017) Fluorescent coumarin-based probe for cysteine and homocysteine with live cell application. Spectrochim Acta A Mol Biomol Spectrosc 183(5)
6. Zivkovic A, Bandolik JJ, Skerhut AJ, Coesfeld C, Zivkovic N, Raos M, Stark H (2017) Introducing students to NMR methods using low-field H-1 NMR spectroscopy to determine the structure and the identity of natural amino acids. J Chem Educ 94(1)
7. Shahrokhian S (2001) Lead phthalocyanine as a selective carrier for preparation of a cysteine-selective electrode. Anal Chem 73(24)
8. Oldiges M, Eikmanns BJ, Blombach B (2014) Application of metabolic engineering for the biotechnological production of L-valine. Appl Microbiol Biotechnol 98(13)
9. Chen W, Zhao Y, Seefeldt T, Guan XM (2008) Determination of thiols and disulfides via HPLC quantification of 5-thio-2-nitrobenzoic acid. J Pharm Biomed Anal 48(5)
10. Inoue T, Kirchhoff JR (2000) Electrochemical detection of thiols with a coenzyme pyrroloquinoline quinone modified electrode. Anal Chem 72(23)
11. Chamsaz M, Arbab-Zavar MH, Akhondzadeh J (2008) Triple-phase single-drop microextraction of silver and its determination using graphite-furnace atomic-absorption spectrometry. Anal Sci 24(6)
12. Niu LY, Chen YZ, Zheng HR, Wu LZ, Tung CH, Yang QZ (2015) Design strategies of fluorescent probes for selective detection among biothiols. Chem Soc Rev 44(17)
13. Cui YJ, Yue YF, Qian GD, Chen BL (2012) Luminescent functional metal-organic frameworks. Chem Rev 112(2)
14. Zhu SJ, Song YB, Zhao XH, Shao JR, Zhang JH, Yang B (2015) The photoluminescence mechanism in carbon dots (graphene quantum dots, carbon nanodots, and polymer dots): current state and future perspective. Nano Res 8(2)
15. Lim SY, Shen W, Gao ZQ (2015) Carbon quantum dots and their applications. Chem Soc Rev 44(1)
16. Sun S, Jiang K, Qian SH, Wang YH, Lin HW (2017) Applying carbon dots-metal ions ensembles as a multichannel fluorescent sensor array: detection and discrimination of phosphate anions. Anal Chem 89(10)
17. Li HT, He XD, Kang ZH, Huang H, Liu Y, Liu JL, Lian SY, Tsang CHA, Yang XB, Lee ST (2010) Water-soluble fluorescent carbon quantum dots and photocatalyst design. Angew Chem Int Ed 49(26)
18. Zhu SJ, Meng QN, Wang L, Zhang JH, Song YB, Jin H, Zhang K, Sun HC, Wang HY, Yang B (2013) Highly photoluminescent carbon dots for multicolor patterning, sensors, and bioimaging. Angew Chem Int Ed 52(14)
19. Li Z, Yu HJ, Bian T, Zhao YF, Zhou C, Shang L, Liu YH, Wu LZ, Tung CH, Zhang TR (2015) Highly luminescent nitrogen-doped carbon quantum dots as effective fluorescent probes for mercuric and iodide ions. J Mater Chem C 3(9)
20. Gupta A., Chaudhary A., Mehta P., Dwivedi C., Khan S., Verma N. C. and Nandi C. K. (2015) Nitrogen-doped, thiol-functionalized carbon dots for ultrasensitive Hg(II) detection. Chem Commun 51(53)
21. Qu SN, Wang XY, Lu QP, Liu XY, Wang LJ (2012) A biocompatible fluorescent ink based on water-soluble luminescent carbon nanodots. Angew Chem Int Ed 51(49)
22. Liu CY, Chang KW, Guo WB, Li H, Shen L, Chen WY, Yan DW (2014) Improving charge transport property and energy transfer with carbon quantum dots in inverted polymer solar cells. Appl Phys Lett 105(7)
23. Zheng M, Ruan SB, Liu S, Sun TT, Qu D, Zhao HF, Xie ZG, Gao HL, Jing XB, Sun ZC (2015) Self-targeting fluorescent carbon dots for diagnosis of brain cancer cells. ACS Nano 9(11)
24. Feng T, Ai XZ, An GH, Yang PP, Zhao YL (2016) Charge-convertible carbon dots for imaging-guided drug delivery with enhanced in vivo cancer therapeutic efficiency. ACS Nano 10(5)
25. Luo PJG, Sahu S, Yang ST, Sonkar SK, Wang JP, Wang HF, LeCroy GE, Cao L, Sun YP (2013) Carbon "quantum" dots for optical bioimaging. J Mater Chem B 1(16)
26. Miao P, Han K, Tang YG, Wang BD, Lin T, Cheng WB (2015) Recent advances in carbon nanodots: synthesis, properties and biomedical applications. Nanoscale 7(5)
27. Yang L, Jiang WH, Qiu LP, Jiang XW, Zuo DY, Wang DK, Yang L (2015) One pot synthesis of highly luminescent polyethylene glycol anchored carbon dots functionalized with a nuclear localization signal peptide for cell nucleus imaging. Nanoscale 7(14)
28. Chen PC, Chen YN, Hsu PC, Shih CC, Chang HT (2013) Photoluminescent organosilane-functionalized carbon dots as temperature probes. Chem Commun 49(16)
29. Xu Q, Kuang TR, Liu Y, Cai LL, Peng XF, Sreeprasad TS, Zhao P, Yu ZQ, Li N (2016) Heteroatom-doped carbon dots: synthesis, characterization, properties, photoluminescence mechanism and biological applications. J Mater Chem B 4(45)
30. Li W, Zhang ZH, Kong BA, Feng SS, Wang JX, Wang LZ, Yang JP, Zhang F, Wu PY, Zhao DY (2013) Simple and green synthesis of nitrogen-doped photoluminescent carbonaceous nanospheres for bioimaging. Angew Chem Int Ed 52(31)
31. Chandra S, Patra P, Pathan SH, Roy S, Mitra S, Layek A, Bhar R, Pramanik P, Goswami A (2013) Luminescent S-doped carbon dots: an emergent architecture for multimodal applications. J Mater Chem B 1(18)
32. Zhang HY, Wang Y, Xiao S, Wang H, Wang JH, Feng L (2017) Rapid detection of Cr(VI) ions based on cobalt(II)-doped carbon dots. Biosens Bioelectron 87
33. Huang S, Yang EL, Yao JD, Liu Y, Xiao Q (2018) Red emission nitrogen, boron, sulfur co-doped carbon dots for "on-off-on" fluorescent mode detection of Ag+ ions and L-cysteine in complex biological fluids and living cells. Anal Chim Acta 1035
34. Dong YQ, Pang HC, Yang HB, Guo CX, Shao JW, Chi YW, Li CM, Yu T (2013) Carbon-based dots Co-doped with nitrogen and sulfur for high quantum yield and excitation-independent emission. Angew Chem Int Ed 52(30)
35. Liu ZX, Chen BB, Liu ML, Zou HY, Huang CZ (2017) Cu(I)-Doped carbon quantum dots with zigzag edge structures for highly efficient catalysis of azide-alkyne cycloadditions. *Green Chem* 19(6)
36. Wang TY, Chen CY, Wang CM, Tan YZ, Liao WS (2017) Multicolor functional carbon dots via one-step refluxing synthesis. Acs Sensors 2(3)
37. Jiang K, Sun S, Zhang L, Wang YH, Cai CZ, Lin HW (2015) Bright-Yellow-Emissive N-doped carbon dots: preparation, cellular imaging, and bifunctional sensing. ACS Appl Mater Interfaces 7(41)
38. Ding H, Wei JS, Zhong N, Gao QY, Xiong HM (2017) Highly efficient red-emitting carbon dots with gram-scale yield for bioimaging. Langmuir 33(44)
39. Reckmeier CJ, Wang Y, Zboril R, Rogach AL (2016) Influence of doping and temperature on solvatochromic shifts in optical spectra of carbon dots. J Phys Chem C 120(19)
40. Liu YH, Duan WX, Song W, Liu JJ, Ren CL, Wu J, Liu D, Chen HL (2017) Red emission B, N, S-co-doped carbon dots for colorimetric and fluorescent dual mode detection of Fe^{3+} ions in complex biological fluids and living cells. ACS Appl Mater Interfaces 9(14)
41. Chen L, Song LP, Zhang YC, Wang P, Xiao ZD, Guo YG, Cao FF (2016) Nitrogen and sulfur codoped reduced graphene oxide as a

general platform for rapid and sensitive fluorescent detection of biological species. ACS Appl Mater Interfaces 8(18)
42. Yang YH, Cui JH, Zheng MT, Hu CF, Tan SZ, Xiao Y, Yang Q, Liu YL (2012) One-step synthesis of amino-functionalized fluorescent carbon nanoparticles by hydrothermal carbonization of chitosan. Chem Commun 48(3)
43. Qian ZS, Ma J, Shan X, Feng H, Shao L, Chen J (2014) Highly luminescent N-doped carbon quantum dots as an effective multifunctional fluorescence sensing platform. Chem Eur J 20(11)
44. Tang ZJ, Lin ZH, Li GK, Hu YL (2017) Amino nitrogen quantum dots-based nanoprobe for fluorescence detection and imaging of cysteine in biological samples. Anal Chem 89(7)
45. Zhao XD, Zhang YZ, Han JM, Jing HM, Gao ZQ, Huang HL, Wang YY, Zhong CL (2018) Design of "turn-on" fluorescence sensor for L-Cysteine based on the instability of metal-organic frameworks. Microporous Mesoporous Mater 268
46. Zhang HY, Feng WY, Feng GQ (2017) A simple and readily available fluorescent turn-on probe for cysteine detection and bioimaging in living cells. Dyes Pigments 139
47. Liu SY, Shi FP, Chen L, Su XG (2013, 19) Tyrosine-functionalized $CuInS_2$ quantum dots as a fluorescence probe for the determination of biothiols, histidine and threonine. Analyst 138
48. Jung M, Kim C, Harrison RG (2018) A dual sensor selective for Hg^{2+} and cysteine detection. Sensors Actuators B Chem 255
49. Hou J, Zhang FS, Yan X, Wang L, Yan J, Ding H, Ding L (2015) Sensitive detection of biothiols and histidine based on the recovered fluorescence of the carbon quantum dots-Hg(II) system. Anal Chim Acta 859
50. Liao S, Zhao XY, Zhu FW, Chen MA, Wu ZL, Song XZ, Yang H, Chen XQ (2018) Novel S, N-doped carbon quantum dot-based "off-on" fluorescent sensor for silver ion and cysteine. Talanta 180
51. Huang H, Weng YH, Zheng LH, Yao BX, Weng W, Lin XC (2017) Nitrogen-doped carbon quantum dots as fluorescent probe for "off-on" detection of mercury ions, L-cysteine and iodide ions. J Colloid Interface Sci 506